sciendo

Management Systems in Production Engineering

2022, Volume 30, Issue 4, pp. 377-387

Date of submission of the article to the Editor: 06/2022
Date of acceptance of the article by the Editor: 10/2022

DOI 10.2478/mspe-2022-0048

ASSESSMENT OF THE STABILITY OF BEV LHD LOADER

Łukasz BOŁOZ
AGH University of Science and Technology

Artur KOZŁOWSKI
Łukasiewicz Research Network – Institute of Innovative Technologies EMAG

Wojciech HORAK
AGH University of Science and Technology

Abstract:
The article concerns the computational model for analysing the stability of the BEV LHD loader. Works were carried out to develop an innovative, light battery-powered loader, which was the subject of an R&D project implemented in cooperation with Bumech S. A. Compared to the existing solutions of loaders with similar load capacity, this one is distinguished by the use of an individual electric drive in each wheel and a replaceable battery. A physical and mathematical model was developed taking into account the specificity of the BEV LHD loader. In the model, the masses of the battery, individual drives, the platform and excavated material are taken into account separately. The developed model allows determining the loader wheel pressure on the floor, depending on the location of its components' centres of gravity, the turning angle of the machine, the amount of excavated material in the bucket and the position of the bucket. The input parameters also include the longitudinal and transverse excavation slope angles. In addition, the model enables determining the inner and outer turning radius of the loader. To verify the theoretical model, dynamic simulation tests were carried out. The results of simulation analyses confirmed the correctness of the developed theoretical model. The model was used to prepare a calculation sheet for analysing the stability on the basis of the adopted parameters. In the article, selected results of the conducted stability analyses have been presented, along with the proposed parameters ensuring the loader's stability. The developed theoretical model enables a quick assessment of the loader's stability, which, due to a number of innovative solutions, differs from existing designs. The structure of the loader at the design stage is subject to numerous modifications, which affect the distribution of the centres of gravity of individual components. The developed model of the loader is a useful, parameterized tool that allows assessing the stability and the values of the turning radii of the machine.

Key words: *self-propelled mining machines, LHD loaders, machine stability, parametric modelling, dynamic simulations, mathematical model, battery power*

INTRODUCTION

LHD (load, haul, dump) loaders are wheel loaders with front dumping buckets. They belong to the most common self-propelled mining machines that are used in the room and pillar mining system in underground mines. What makes them different from conventional loaders is their low height, which allows reaching places with a very low roof. One of the major elements of the LHD loader is a rear body *1* seated on an oscillation axle 5 (Figure 1a). Between the rear body *1* and the oscillation axle *5* there is a joint *6* with a horizontal axis (Figure 1b). The articulated oscillation axle is responsible for the ability to ride on an uneven surface, as shown in Figure 1c. The rear body *1* is connected to the platform *2* by means of a joint *4* with a vertical axis. The articulated connection of the rear body and the platform with hydraulic cylinders is responsible for the turning of the machine. The bucket *3* is attached to the platform *2*. The bucket *3* is attached by means of a suitable kinematic system that allows it to be lifted and rotated. The Z and T systems shown in Figure 1d are the most commonly used.

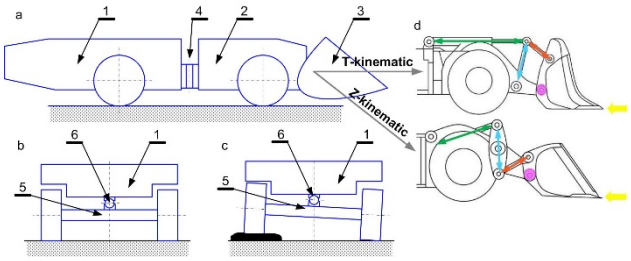

Fig. 1 Diagram of the construction of the articulated LHD loader of the drilling rig:
a. general view of the machine from above,
b. rear view of the rear body with an oscillation axle,
c. ride on an uneven surface
d. kinematic systems T and Z (Fig. d from [1])

The LHD loader, due to the necessity of crossing the junctions of headings, turns in the joint by an angle of up to 42°. Such a machine is stable when its centre of gravity (blue point) is inside the triangle (red lines) defined by the centres of the front wheels and the rear axis centre (Figure 2a). The lines connecting these points are called the tipping edges. When the machine is turning, the centre of the rear axis shifts, and at the same time, the resultant centre of gravity of the machine moves significantly towards the tipping edge, reducing the machine's stability (Figure 2b). Therefore, at the design stage, it is necessary to control the position of the centre of gravity, taking into account the full turn of the machine, the position of the bucket as well as the longitudinal and transverse inclination of the working.

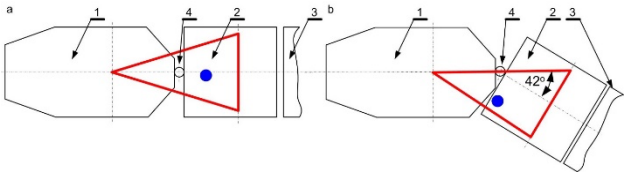

Fig. 2 Condition for articulated LHD loader stability (description as before):
a. ride straight ahead, b. maximum turn

The article is devoted to a light battery-operated LHD loader with the designation EV-LKP1, which is the subject of the project carried out in cooperation with Bumech S. A. The EV-LKP1 loader with a total weight of 20,000 kg, including a capacity of 4,000 kg, is intended for use particularly in underground mines. It is a BEV (battery electric vehicle) loader. Battery-powered LHD loaders have been available on the market for several years, for example the A4 model from Artisan and the L140B model from Aramine (Figure 3). The A4 loader has a capacity of 4,000 kg, while the L140B model is the smallest battery-operated loader on the market with a capacity of merely 1,300 kg. The largest underground battery-operated LHD loaders have a load capacity of 14,000 kg (ST14 produced by Epiroc) and even 18,000 kg (LH518B produced by Sandvik).
The EV-LKP1 loader, compared to existing solutions with similar load capacity, is distinguished by the use of an individual electric drive in each wheel (in-wheel-drive) and has a removable energy storage (battery swap). An important aspect of this loader operation is the possibility of quick battery replacement, thanks to which energy storage discharge results merely in a short maintenance break and the loader can quickly resume its work. The design of the loader drive system makes it possible to recover energy when the machine is braking and going down a hill, which may translate into an extended working time between subsequent battery swaps. The design solutions used in the discussed loader require the development of appropriate computational models to assess the loader's stability at each stage of design.

Fig. 3 Selected models of BEV LHD loaders (Artisan A4 model, Aramine L140B model)

LITERATURE REVIEW

LHD loaders are widely used in underground mining. In recent years, an accelerated development in mining machines construction, including LHD loaders, has been observed, especially in the field of battery power, support systems, remote control and work autonomy.
Currently, modern methods and tools are used to design and test working machines, including mining machines. In various scientific and research centers, work is carried out on the wear of cutting tools [2], bolt load [3, 4], mining methods [5] or dynamic simulations, etc. [6, 7, 8, 9].
CAD/CAE programmes are applied, theoretical models and tests stands are developed The works concern calculations and testing of an artificial bottom of a mining shaft [10], the use of neural networks in simulations [11], numerical simulations of the mining process [12] or numerical analyzes according to appropriate standards [13].
More and more attention is paid to ergonomics and occupational safety [14]. A growing number of new solutions of machines and machine elements are being developed You can find articles of mechanized roadway supports [15], battery-powered machines [16], mulchers [17], mining automation and robotization [18] or automatic drilling rigs for mining and tunnelling [19].
From the beginning of the process of designing this type of machine, especially an articulated one, it is necessary to analyse the values of mass and the location of the centres of gravity of the key components in order to assess the stability of the entire machine. Stability is influenced by the longitudinal and transverse inclination of the excavation, the turning angle of the machine body, the position of the bucket as well as the amount and manner of distribution of the excavated material. Currently, there are no theoretical models enabling a quick analysis and assessment of the stability of so designed machines. Simulation tests can be done using CAD/CAE tools. However, such tests are time-consuming and require the develop-

ment of appropriate models for each machine, which limits the possibility of conducting a comprehensive analysis for many variants of parameters in a short time.

Information on the machine's stability can be obtained from empirical tests on truck scales and from test runs. Practice shows that the minimum load from mass forces of one wheel on the ground of more than 1,000 kg guarantees stability of this type of machines in a horizontal excavation. Such measurements, however, can only be carried out for a ready-made machine, and the model described in the article is used at the stage of designing a unique LHD loader.

The stability of various types of working machines is a well-known problem, which has been described in the subject literature. The problem of tipping stability comes down to the analysis of the location of the machine's centre of gravity in relation to the tipping edge [20]. Machines typically prone to overturning, such as cranes, are frequently the subject of research and articles [21, 22, 23, 24]. However, these are design solutions with different operational characteristics than LHD vehicles, which usually work after prior levelling and in a stationary manner. In the case of cranes, the tipping moments and the stabilizing moment as well as the tipping stability coefficient are calculated. It is therefore not necessary to calculate the load of mass forces at specified points.

As regards the analysis of vehicle stability, the subject literature provides general theoretical models for the four-wheel chassis itself [25] or for vehicles with multiple axes [26]. One of the articles discusses an interesting articulated machine, but on a caterpillar chassis, for which the Authors presented a complex dynamic theoretical model and the results of analytical research [27].

Many studies concern agricultural machines, articulated and with rigid frames. Such machines must also be assessed in terms of stability due to their work in a terrain with longitudinal and transverse slopes. For this purpose, both static and dynamic models as well as the results of empirical research are used [29, 30].

As regards articulated mining machines, a number of works related to drilling rigs and bucket loaders can be indicated. One of the articles describes a comprehensive model with a spreadsheet for analysing the stability of two-boom drilling rigs [31]. The authors verified and validated the developed model using various methods, including a comparison of the results with the results of empirical research. Another article is concerned with working machines' tipping stability, with a focus on various solutions of bucket loaders [32]. The authors concentrated on the proprietary test stand enabling empirical assessment of stability and verification of theoretical models. This stand allows simulating the inclination of an articulated machine model while measuring the pressure of the wheels on the ground. In another article, the same authors conducted a comprehensive study of the loader stability and developed their own theoretical model. As a result, they proposed changes positively influencing the stability of the articulated wheel loader [33].

Similarly, another team studied the stability of an articulated bucket loader in several subsequent articles [34, 35, 36]. Various dynamic models and several versions of the loader in scale were developed. The results obtained from the theoretical models were verified by the test results. In addition to typical situations, a ride over obstacles of various shapes and sizes was also analysed.

Due to the use of battery swap and drive replacement in each wheel, it was necessary to develop a dedicated computational model enabling a quick analysis of the machine's stability. The application of models known from the subject literature was not sufficient. The loader undergoes frequent modifications at the design stage, and each change in the geometry, mass or position of the centre of gravity of its components is analysed in terms of stability.

METHODOLOGY OF RESEARCH

The aim of the work in question was to develop a computational model and a spreadsheet for assessing the stability of the new solution of the BEV LHD loader. In the first step, a physical model of the machine was developed based on the analysis of the existing LHD loaders while taking into account new design solutions. A number of assumptions were specified, and, next, the physical model was expressed in the form of a mathematical model. A static computational model was created. The model was saved as a transparent spreadsheet in the MathCad Prime Express programme. Then, the developed model was verified using the Dynamic Simulation module in the Autodesk Inventor Professional environment. The subject of the research is a unique LHD loader, which is currently being designed, therefore it is not possible to use empirical research. The developed spreadsheet was used to evaluate the stability of various variants of the EV-LKP1 loader. Next, parameter values guaranteeing the stability of the machine, regardless of the turning angle, inclination or the amount of excavated material in the bucket, were proposed. In order to facilitate the interpretation of the results and due to the typically practical nature of the model, all calculations were performed using weights expressed in kilograms. So in the article "force" or "pressure" mean load from mass forces.

PHYSICAL AND MATHEMATICAL MODEL OF THE LHD LOADER

Due to the need to develop an analytical model allowing a quick assessment of the LHD loader's stability, a number of assumptions were specified. The model must enable calculating the wheel pressure on the ground in horizontal and inclined excavations, as a function of a number of parameters. The model was developed for an articulated machine with an oscillation axle on a wheel chassis. According to the design, the machine can move in workings with a maximum longitudinal slope of ± 17° and a transverse slope of ± 5°. Determining the location of the centre of gravity of the LHD loader requires its mass to be distributed into individual components that perform relative motion.

In the first step, the loader was divided into four masses: rear body, oscillation axle, platform, bucket. Such a model turned out to be insufficient. The use of a battery swap and replaceable drive in each wheel required detailed analyses. The influence of the change of the drive system's mass as well as the lack of energy storage on the machine's stability had to be taken into account independently. Therefore, a detailed theoretical model was developed, divided into seven components represented by point masses (Figure 4). Two variants were considered – one with a battery installed at the end of the machine, and the other – in the middle of it. In both versions, the removable energy storage is related to the rear body. Preliminary simulations revealed that it was sufficient to separate the front drive's mass from the mass of the platform and to assume the weight of the oscillation axle together with the rear drive. The machine was divided into the following components:

m_t – rear body mass without oscillation axle and battery,
m_k – mass of oscillation axle with rear drive,
m_b – battery mass with housing,
m_p – platform mass without front drive,
m_n – front drive mass,
m_l – bucket mass,
m_u – excavated material mass.

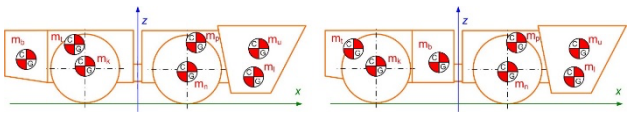

Fig. 4 Division of the loader into seven-point masses in two variants (description in the text)

The most important geometrical parameters are the distances between the wheels and the machine's joint as well as the quantities describing the position of the bucket with excavated material. In addition, the machine turning angle and a change in the position of the bucket with excavated material both vertically and horizontally should be taken into account (Fig. 5).

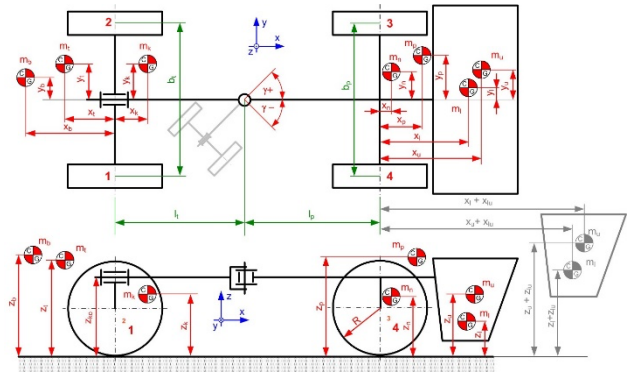

Fig. 5 Values adopted for the computational model (description in the text)

Machine geometry:
b_p – front wheel track,
l_p – front axis distance,
b_t – rear wheel track,
l_t – rear axis distance,
z_{ko} – height of oscillation axle joint,
R – outer radius of the tyre in free condition,
Values of masses of the centres of gravity:
m_t – rear body mass without oscillation axle and battery,
m_k – oscillation axle with rear drive,
m_b – battery mass with housing,
m_p – platform mass with front drive,
m_n – front drive mass,
m_l – bucket mass,
m_u – excavated material mass.
Local coordinates of the centres of gravity:
x_t, y_t, z_t – position of the centre of gravity of the rear body without oscillation axle and battery,
x_k, y_k, z_k – position of the centre of gravity of the oscillation axle with rear drive,
x_b, y_b, z_b – position of the centre of gravity of the battery with housing,
x_p, y_p, z_p – position of the centre of gravity of the platform,
x_p, y_p, z_p – position of the centre of gravity of the platform without front rear,
x_n, y_n, z_n – position of the centre of gravity of the front drive,
x_l, y_k, z_k – position of the centre of grvity of the bucket,
x_u, y_u, z_u – position of the centre of gravity of the excavated material.
Machine variables:
γ – machine turning angle (positive angle to the right, negative angle to the left),
x_{lu}, z_{ku} – bucket forward and upward movement,
y_u – assymetry of excavated material in the bucket.
The plus sign of the coordinates was used as shown in the figure; if the centre of gravity was on the other side of the axis, the minus sign was applied. This enabled simulating an alternative position of individual centres of gravity, which was used to analyse the battery mounted to the rear body at the end of the machine and in the middle of the machine, between the rear axis and the joint of the machine.
The specified geometric parameters have been described in the diagrams in a way facilitating their accurate and easy determination. The coordinates of the centres of gravity as well as the cooridnates of the wheel centres and the oscillation axle change depending on the chassis turning angle and the position of the bucket. For the purpose of analysing the entire loader, it is necessary to assign the values of *x, y, z* coordinates in the global system.
Given the construction of the machine, the centre of the coordinate system was related to the platform, and its origin was assumed to be in the joint at the floor level. Therefore, formulas for coordinates in the global system were derived. In the formulas, the previously adopted subscripts with an additional designation *„c"* were applied. In addition to the previously adopted subscripts, wheel numbers *„x"* from 1 to 4 were also assigned with the *„x_0"* coordinate for the oscillation axle. The location of the global system and the way of marking the coordinates are shown in green for several selected centres of gravity in Figure 6.

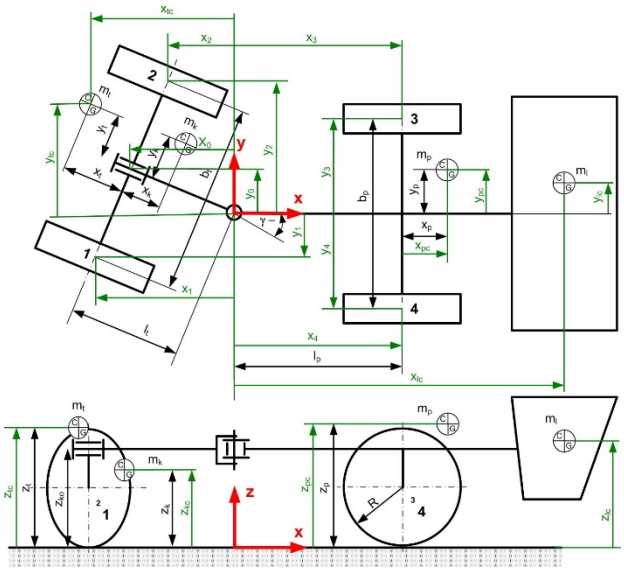

Fig. 6 Selected x, y, z global coordinates of the machine

The equations enabling determination of the global coordinates for the analysed case are presented below. They were derived using standard transformations and formulas for vector transformations and rotations.

Coordinates of the centre of gravity of the rear body:

$$x_{tc} = -(l_t + x_t) \cdot cos(\gamma) - y_t \cdot sin(\gamma) \quad (1)$$

$$y_{tc} = -(l_t + x_t) \cdot sin(\gamma) + y_t \cdot cos(\gamma) \quad (2)$$

$$z_{tc} = z_t \quad (3)$$

Coordinates of the centre of gravity of the oscillation axle with drives:

$$x_{kc} = -(l_t + x_k) \cdot cos(\gamma) - y_k \cdot sin(\gamma) \quad (4)$$

$$y_{kc} = -(l_t + x_k) \cdot sin(\gamma) + y_k \cdot cos(\gamma) \quad (5)$$

$$z_{kc} = z_k \quad (6)$$

Coordinates of the battery's centre of gravity:

$$x_{bc} = -(l_t + x_b) \cdot cos(\gamma) - y_b \cdot sin(\gamma) \quad (7)$$

$$y_{bc} = -(l_t + x_b) \cdot sin(\gamma) + y_b \cdot cos(\gamma) \quad (8)$$

$$z_{bc} = z_b \quad (9)$$

Coordinates of the platform's centre of gravity:

$$x_{pc} = l_p + x_p \quad (10)$$

$$y_{pc} = y_p \quad (11)$$

$$z_{pc} = z_p \quad (12)$$

Coordinates of the centre of gravity of the front drive:

$$x_{nc} = l_p + x_n \quad (13)$$

$$y_{nc} = y_n \quad (14)$$

$$z_{nc} = z_n \quad (15)$$

Coordinates of the bucket's centre of gravity:

$$x_{lc} = l_p + x_l + x_{lu} \quad (16)$$

$$y_{lc} = y_l \quad (17)$$

$$z_{lc} = z_l + z_{lu} \quad (18)$$

Coordinates of the excavated material's centre of gravity:

$$x_{uc} = l_p + x_u + x_{lu} \quad (19)$$

$$y_{uc} = y_u \quad (20)$$

$$z_{uc} = z_u + z_{lu} \quad (21)$$

Coordinates of the location of the contact of the wheel marked with number 1:

$$x_1 = -l_t \cdot cos(\gamma) + \frac{b_t}{2} \cdot sin(\gamma) \quad (22)$$

$$y_1 = -l_t \cdot sin(\gamma) - \frac{b_t}{2} \cdot cos(\gamma) \quad (23)$$

Coordinates of the location of the contact of the wheel marked with number 2:

$$x_2 = -l_t \cdot cos(\gamma) - \frac{b_t}{2} \cdot sin(\gamma) \quad (24)$$

$$y_2 = -l_t \cdot sin(\gamma) + \frac{b_t}{2} \cdot cos(\gamma) \quad (25)$$

Coordinates of the location of the contact of the wheel marked with number 3:

$$x_3 = l_p \quad (26)$$

$$y_3 = \frac{b_p}{2} \quad (27)$$

Coordinates of the location of the contact of the wheel marked with number 4:

$$x_4 = l_p \quad (28)$$

$$y_4 = -\frac{b_p}{2} \quad (29)$$

Coordinates of the location of the oscillation axle (marked with number „0"):

$$x_0 = -l_t \cdot cos(\gamma) \quad (30)$$

$$y_0 = -l_t \cdot sin(\gamma) \quad (31)$$

The values of global coordinates allow deriving formulas for the location and mass of the centre of gravity of the loader. The mass of the oscillation axle with the rear wheel, which is a separate element in the calculations, was ignored in the formulas quoted below. The centre of gravity of the loader without the oscillation axle can be calculated from the following formulas:

$$x_{cbk} = \frac{m_t \cdot x_{tc} + m_b \cdot x_{bc} + m_p \cdot x_{pc} + m_n \cdot x_{nc} + m_l \cdot x_{lc} + m_u \cdot x_{uc}}{m_t + m_b + m_p + m_n + m_l + m_u} \quad (32)$$

$$y_{cbk} = \frac{m_t \cdot y_{tc} + m_b \cdot y_{bc} + m_p \cdot y_{pc} + m_n \cdot y_{nc} + m_l \cdot y_{lc} + m_u \cdot y_{uc}}{m_t + m_b + m_p + m_n + m_l + m_u} \quad (33)$$

$$z_{cbk} = \frac{m_t \cdot z_{tc} + m_b \cdot z_{bc} + m_p \cdot z_{pc} + m_n \cdot z_{nc} + m_l \cdot z_{lc} + m_u \cdot z_{uc}}{m_t + m_b + m_p + m_n + m_l + m_u} \quad (34)$$

$$m_{cbk} = m_t + m_b + m_p + m_n + m_l + m_u \quad (35)$$

Next, the load acting on the machine's joint should be calculated in order to determine the values of the wheels' pressure (load from mass forces) in a horizontal excavation:

$$m_0 = \frac{x_3 - x_{cbk}}{x_3 - x_0} \cdot m_{cbk} \quad (36)$$

The values of the load from mass forces of individual wheels on the floor, expressed in mass, can be calculated from the following formulas:

$$m_1 = m_k + m_0 - m_2 \quad (37)$$

$$m_2 = \frac{m_0 \cdot (y_0 - y_1) + m_k \cdot (y_{kc} - y_1)}{y_2 - y_1} \quad (38)$$

$$m_3 = \frac{m_{cbk} \cdot (y_{cbk} - y_4) - m_0 \cdot (y_0 - y_4)}{y_3 - y_4} \quad (39)$$

$$m_4 = m_{cbk} - m_0 - m_3 \quad (40)$$

The excavation may be inclined: longitudinally – longitudinal slope angle α or transversely – transverse slope angle β. The transverse and longitudinal angles are measured in directions that are perpendicular in relation to each other, relative to the vertical (Figure 7). The *xyz* system is a local system related to the centre of gravity of the

analysed self-propelled mining machine. Due to the limited values of the longitudinal ($\alpha \leq \pm 17°$) and transverse ($\alpha \leq \pm 5°$) angles, simplified calculations were applied.

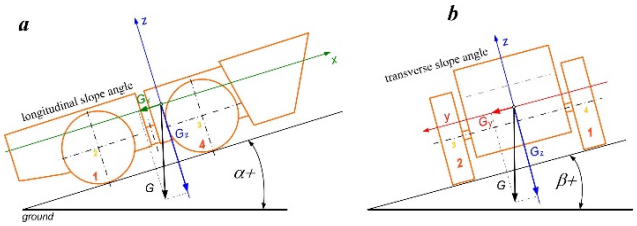

Fig. 7 Diagram for determining the distribution of the force of gravity in an excavation inclined:
a. longitudinally α > 0 and transversely β = 0,
b. transversely β > 0 and longitudinally α = 0

Based on the analysis of the distribution of gravitational force, the formulas for its individual components were expressed as follows:

$$G_x = G\,sin(\alpha) \tag{41}$$

$$G_y = G\,sin(\beta) \tag{42}$$

$$G_z = G\sqrt{cos^2(\alpha) - sin^2(\beta)} \quad \text{or} \quad G_z = G\sqrt{cos^2(\beta) - sin^2(\alpha)} \tag{43}$$

$$WG = \sqrt{cos^2(\beta) - sin^2(\alpha)} \rightarrow G_z = G \cdot WG \tag{44}$$

An excavation with a longitudinal and transverse slope requires developing further formulas to calculate the wheel pressure on the floor. Taking into consideration both inclinations simultaneously, the components of the gravity force of the oscillation axle and the rest of the machine can be expressed as:

$$m_{cbkx} = m_{cbk} \cdot sin(\alpha) \tag{45}$$

$$m_{cbky} = m_{cbk} \cdot sin(\beta) \tag{46}$$

$$m_{cbkz} = m_{cbk} \cdot WG \tag{47}$$

$$m_{kx} = m_k \cdot sin(\alpha) \tag{48}$$

$$m_{ky} = m_k \cdot sin(\beta) \tag{49}$$

$$m_{kz} = m_k \cdot WG \tag{50}$$

Knowing the components of gravitational force that load the machine, one can write formulas for the load components acting the joint:

$$m_{0y} = \frac{m_{cbky} \cdot (x_3 - x_{cbk})}{x_3 - x_0} \tag{51}$$

$$m_{0z} = \frac{m_{cbkz} \cdot (x_3 - x_{cbk}) + m_{cbkx} \cdot z_{cpw}}{x_3 - x_0} \tag{52}$$

The above dependencies can be used to calculate the load of mass forces of wheel pressure on the ground, expressed in mass:

$$m_{1n} = m_{kz} + m_{0z} - m_{2n} \tag{53}$$

$$m_{2n} = \frac{m_{0z} \cdot (y_0 - y_1) + m_{kz} \cdot (y_{kc} - y_1) + m_{ky} \cdot z_{kc} + m_{0y} \cdot z_{ko}}{y_2 - y_1} \tag{54}$$

$$m_{3n} = \frac{m_{cbkz} \cdot (y_{cpw} - y_4) + m_{cbky} \cdot z_{cbk} - m_{0y} \cdot z_{cbk} - m_{0z} \cdot (y_0 - y_y)}{y_3 - y_4} \tag{55}$$

$$m_{4n} = m_{cbkz} - m_{0z} - m_{3n} \tag{56}$$

The key operational parameter of self-propelled articulated mining machines is the inner and outer turning radius. Therefore, additional formulas enabling its calculation were derived on the basis of the developed diagram, which is presented in Figure 8.

The value of the turning radii depends on the geometry and the turning angle of the machine. Depending on the specific values, the minimum turning radius of the loader can be limited by the front or rear part of the machine.
To determine the turning radii, it is necessary to take into account the additional parameters presented in Figure 8:
R_w – inner turning radius,
R_{zt} – outer turning radius resulting from the rear part of the machine
R_{zp} – outer turning radius resulting from the front part of the machine,
b_c – machine width,
b_l – bucket width,
l_{tc} – distance from the joint to the end of the rear part,
l_{pc} – distance from the joint to the end of the front part,
γ_p – auxiliary angle,
l_{pt} – auxiliary length.

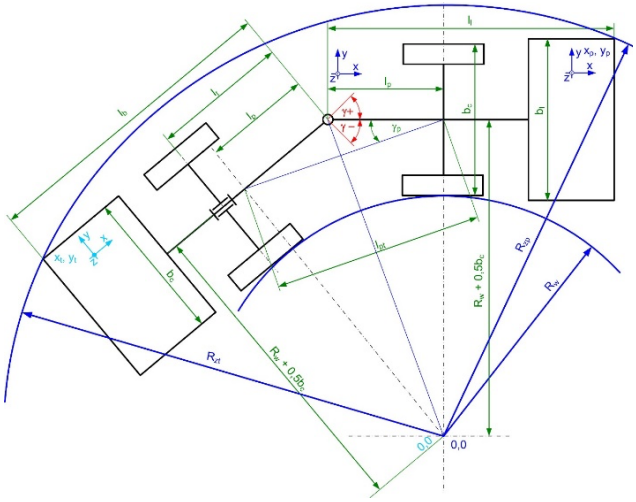

Fig. 8 Diagram for determining the turning radii of the LHD loader (description in the text)

The developed diagram was used to derive formulas for subsequent parameters, including the turning radii:

$$l_{pt} = l_p\sqrt{2(1 + cos(-|\gamma|))} \tag{57}$$

$$\gamma_p = a\,sin\left(\frac{l_p \cdot sin\,|\gamma|}{l_{pt}}\right) \tag{58}$$

$$R_w = l_p \cdot cot(\gamma_p) - \frac{b_c}{2} \tag{59}$$

$$R_{zp} = \sqrt{(l_{pc} - l_p)^2 + \left(R_w + \frac{b_c + b_l}{2}\right)^2} \tag{60}$$

$$R_{zt} = \sqrt{(-l_{tc} + l_p)^2 + (R_w + b_c)^2} \tag{61}$$

VALIDATION OF THE ANALYTICAL MODEL BY MEANS OF SIMULATION TESTS

The developed computational model was verified by comparing the results with the results of model studies conducted in the Autodesk Inventor Professional environment, in the Dynamic Simulation module. A virtual, simplified model of the machine was developed (Figure 9a) and multi-variant simulations were carried out to check the values of wheel pressure on the floor, depending on the parameters describing the structure and the turning

angle of the machine. The set parameters were: machine geometry, values of the subassemblies' masses, location of the centre of gravity of the subassemblies and the angle of longitudinal and transverse inclination of the excavation. The angle of inclination in the virtual environment was simulated by changing, respectively, the *x, y, z* components of gravitational acceleration acting on the system. Sample results of wheel pressure forces during the turning of the loader have been shown in Figure 9 b

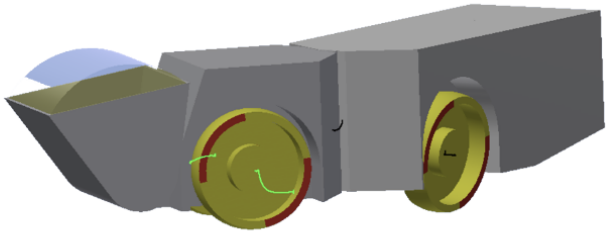

a)

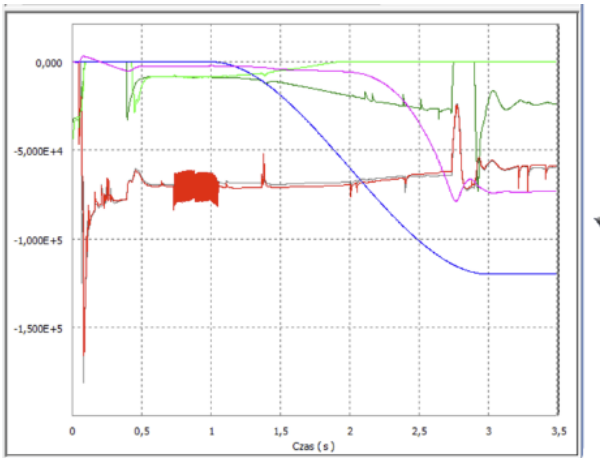

b)

Fig. 9 a) Virtual model of the LHD loader, b) sample results of stability tests

ASSESSMENT OF THE STABILITY OF THE BEV LHD LOADER

The designed LHD loader is characterized by a number of new solutions, which result from the use of a removable energy storage and the installation of drive motors in each of the wheels. At the design stage, several variants of this machine were developed, therefore it was necessary to constantly verify their stability and analyse the possible turning radii. A calculation spreadsheet was developed so as to assess individual variants of the loader design based on the previously discussed parameters regarding the individual masses and geometrical dimensions of the machine.

The results of multivariate simulations show that the greatest impact on the stability of the modelled vehicle is exerted by the location of the energy storage, which is the consequence of both its dimensions and significant mass. Initially, the plan was to locate it in the rear part of the machine, behind the operator. However, the results of preliminary stability analyses showed that for the adopted design assumptions and the assumed operational parameters of the designed loader, location in the middle part of the machine was more advantageous. It was therefore proposed to place the energy storage between the rear axis and the loader joint. The subject of the analyses presented in this paper will be this version of the loader. Figure 10 shows two selected variants of the EV-LKP1 loader with a battery at the end (I) and in the middle of the machine (II).

The results of stability and turning radius tests for variant (I) have been presented in Table 1, Table 2 and Figure 11. In this variant, the machine positioned straight ahead is stable for the situation with excavated material, without excavated material and without the battery. On the other hand, if the turning angle reaches approximately 30°, the machine loses stability only in the case of an empty bucket, and for a turn by ca 40° – also a full bucket. The input parameters for the model are presented in Tables 3-6. Variant (II) and other variants are calculated in the same way.

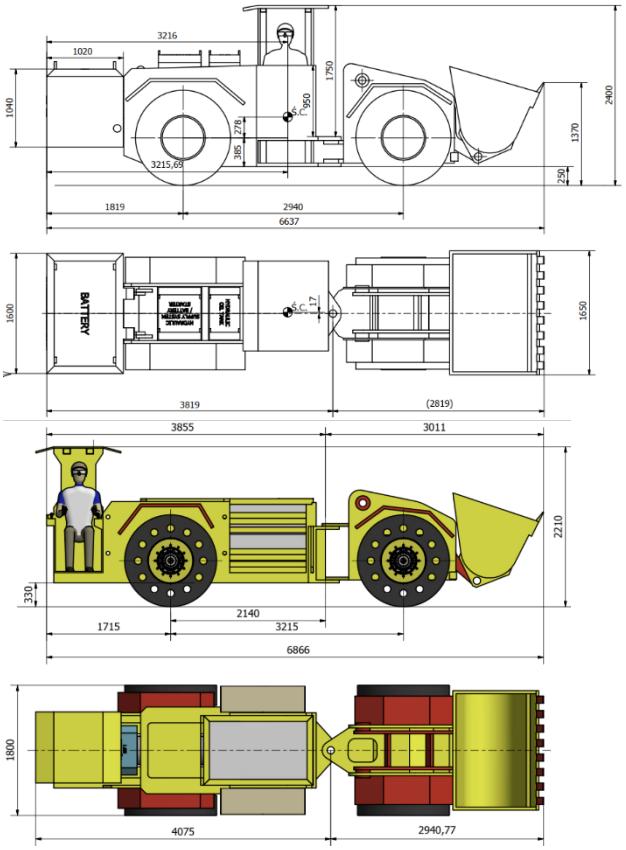

Fig. 10 Two selected variants of the EV-LKP1 loader with a battery at the end (I) and in the middle of the machine (II)

Table 1
Results of stability tests for variant (I) during a ride straight ahead

	Full bucket (4000 kg)		Empty bucket		Empty bucket without battery	
	weight [kg]	share %	weight [kg]	share %	weight [kg]	share %
Wheel 1	5 579	29%	6 368	41%	4 923	37%
Wheel 2	5 579	29%	6 368	41%	4 923	37%
Wheel 3	4 302	22%	1 514	10%	1 959	15%
Wheel 4	3 940	20%	1 151	7%	1 596	12%
Total	19 400	100%	15 401	100%	13 401	100%
Front axis	8 242	42%	2 665	17%	3 555	27%
Rear axis	11 158	58%	12 736	83%	9 846	73%

Table 2
Results of stability and turning radii tests for variant (I) with a turning angle of 30° and 40°

	Turn α = 30°				Turn α = 40°			
	Full bucket		Empty bucket		Full bucket		Empty bucket	
	weight [kg]	share %	weight [kg]	share %	weight [kg]	share %	weight [kg]	share %
Wheel 1	5 415	28%	6 283	41%	5 259	27%	6 197	40%
Wheel 2	5 415	28%	6 283	41%	5 259	27%	6 197	40%
Wheel 3	1 093	6%	-325	-2%	-60	0%	-984	-6%
Wheel 4	7 477	39%	3 160	21%	8 942	46%	3 990	26%
Front axis	8 570	44%	2 835	18%	8 882	46%	3 006	20%
Rear axis	10 830	56%	12 566	82%	10 518	54%	12 394	80%
	Radius [mm]:	**Rw**	**Rzp**	**Rzc**	**Radius [mm]:**	**Rw**	**Rzp**	**Rzc**
		2 708	4 723	5 182		1 783	3 891	4 442

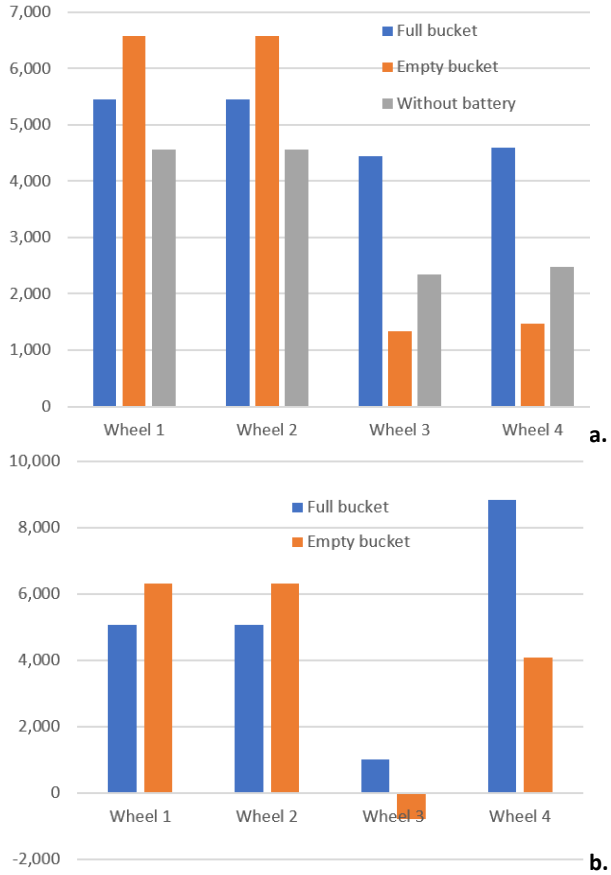

Fig. 11 Sample results of stability tests for variant (I): a. ride straight ahead, b. machine turn by 30°

Table 3
Geometrical values of the EV-LKP1 loader – ariant (I)

No.	Parameter	Designation	Value [mm]
1.	Front wheel track	b_p	1200
2.	Front axis distance	l_p	940
3.	Rear wheel track	b_t	1200
4.	Rear axis distance	l_t	1128
5.	Oscillation axle joint height	z_{ko}	800
6.	Wheel outer diameter	R	625

Table 4
Weight of the EV-LKP1 loader subassemblies – variant (I)

No.	Subassembly	Designation	Value [kg]
1.	Rear body without oscillation axle assembly	m_t	8 000
2.	Platform	m_p	5 000
3.	Oscillation axle assembly	m_k	2 000
4.	Bucket with excavated material	m_l	1 000 ÷ 5 000

Table 5
Location of the centres of gravity of the EV-LKP1 loader subassemblies – variant (I)

No.	Subassembly	Designation	x [mm]	y [mm]	z [mm]
1.	Rear body without oscillation axle assembly	x_t, y_t, z_t	990	0	990
2.	Platform	x_p, y_p, z_p	-370	0	780
3.	Oscillation axle assembly	x_k, y_k, z_k	0	0	625
4.	Bucekt with excavated material	x_l, y_l, z_l	1250	0	940

Table 6
Variables of the EV-LKP1 loader subassemblies – variant (I)

No.	Parameter	Designation	Range
1.	Machine turning angle	α	-40° ÷ +40°
2.	Bucket lifting	z_l	940 mm
3.	Bucket extension	x_l	1250 mm
4.	Uneven load of bucket	y_l	0 mm ÷ ± 450 mm

RESULTS OF RESEARCH

As a result of the analysis of many variants, differing not only in the location of the battery but also in the wheelbase, wheel track and the location of important heavy elements, the researchers proposed several sets of the EV-LKP1 loader parameters that allow obtaining full stability regardless of the operating conditions.

One of the proposed solutions is based on the geometry of variant (I) presented in Tables 3-6. New positions of the centres of gravity were determined – they are presented in Table 7.

Table 7
Proposed positions of the centres of gravity of the EV-LKP1 loader

No.	Subassembly	Designation	x [mm]	y [mm]	z [mm]
1.	Rear body without oscillation axle assembly	$m_t - x_t, y_t, z_t$	100	0	990
2.	Platform	$m_p - x_p, y_p, z_p$	-100	0	780
3.	Oscillation axle	$m_k - x_k, y_k, z_k$	0	0	625
4.	Bucket with excavated material	$m_l - x_l, y_l, z_l$	1250	0	940

This data was used in stability tests, the results of which have been given in Table 8 and Figure 12.

The results clearly indicate the full stability of the machine. It may be difficult in practice to achieve the proposed positions of the centres of gravity. However, the presented values allow achieving a pressure force distribution of 40/60 and 60/40, respectively, for the machine with a full and an empty bucket. The distribution values commonly found in practice are 20/80 and 80/20, so the centre of gravity of the rear body in the discussed design can be significantly shifted to the rear of the machine.

Table 8
Results of stability tests for the variant with the proposed positions of the centres of gravity

	Ride straight ahead α = 0°				Full turn α = 40°			
	Empty bucket		Full bucket		Empty bucket		Full bucket	
	weight [kg]	share %	weight [kg]	share %	weight [kg]	share %	weight [kg]	share %
Wheel 1	5 012	31%	3 803	19%	4 962	31%	3 576	18%
Wheel 2	5 012	31%	3 803	19%	4 962	31%	3 576	18%
Wheel 3	2 988	19%	6 197	31%	2 564	16%	4 275	21%
Wheel 4	2 988	19%	6 197	31%	3 512	22%	8 573	43%
Front axis	*5 976*	*37%*	*12 394*	*62%*	*6 076*	*38%*	*12 848*	*64%*
Rear axis	*10 024*	*63%*	*7 606*	*38%*	*9 924*	*62%*	*7 152*	*36%*

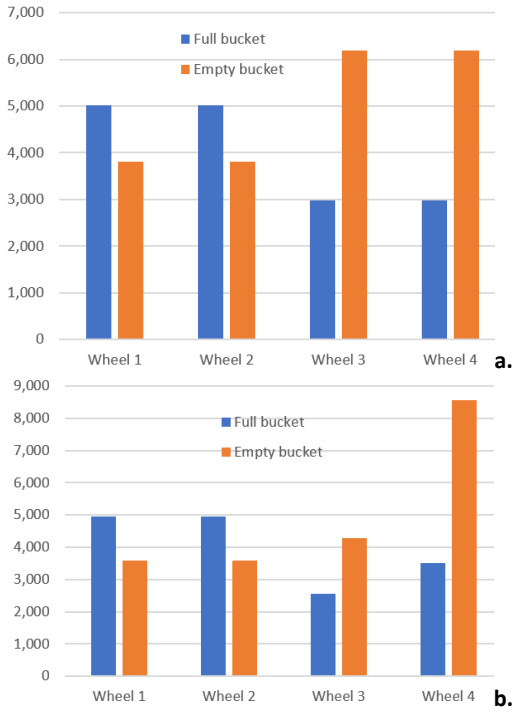

Fig. 12 Results of stability tests for the variant with the proposed positions of the centres of gravity:
a. ride straight ahead,
b. machine turn 40°

CONCLUSIONS

Mining machines, similarly to machines used in many other industries, are undergoing transformation, especially in the field of electric power supply as well as remote

and autonomous work. Currently, nearly all mining machines typically equipped with combustion engines have their electric, battery-powered counterparts. The use of battery power is not only a change in the drive system design, but also a significant change in weight distribution. This is of key importance for articulated machines, such as LHD loaders, due to the need to ensure the stability of the machine. The currently designed unique EV-LKP1 loader required developing an appropriate computational model for quick verification of the wheel pressure on the ground and the assessment of possible turning radii. The developed model and spreadsheet were verified by simulation tests in a virtual environment, which confirmed their correctness. The sheet is used for stability control in the process of designing the EV-LKP1 loader. The conducted research has demonstrated that seemingly small changes frequently result in a loss of stability when the machine is turning or when the bucket is empty. The loader design is currently underway. However, after it has been completed and the machine constructed, empirical tests will be carried out in order to further verify the developed model.

The conducted analysis involved verifying many variants and developing several sets of parameters ensuring the machine's full stability. The developed model and the parameterized calculation sheet are valuable, useful engineering tools that can be applied for analysing BEV LHD loaders and other articulated vehicles.

FUNDING

The project entitled „Innovative EV-LKPI vehicle for loading loose materials" co-financed by the European Regional Development Fund in accordance with the agreement POIR.01.01.01-00-1427/20-00.

REFERENCES

[1] Solid as a rock, GHH group, https://ghhrocks.com, access: 24.08.2022.

[2] V. David, J. Gajewski, M. Forbelská, Z. Vintr and J. Jonak, "Drilling head knives degradation modelling based on stochastic diffusion processes backed up by state space models", *Mechanical Systems and Signal Processing*, 166, 2022.

[3] K. Skrzypkowski, "Case Studies of Rock Bolt Support Loads and Rock Mass Monitoring for the Room and Pillar Method in the Legnica-Głogów Copper District in Poland", *Energies*, 13, 2998, pp. 1-20, 2020.

[4] K. Skrzypkowski, W. Korzeniowski, K. Zagórski and A. Zagórska, "Adjustment of the Yielding System of Mechanical Rock Bolts for Room and Pillar Mining Method in Stratified Rock Mass", *Energies*, 13, 2082, pp. 1-20, 2020.

[5] K. Kotwica, and P. Małkowski, "Methods of Mechanical Mining of Compact-Rock – A Comparison of Efficiency and Energy Consumption", *Energies*, 12, 3562, pp. 1-25, 2019.

[6] J. Joostberens, A. Pawlikowski, D. Prostański and K. Nieśpiałowski, "Method for Assessment of Operation of Analog Filters Installed in the Measuring Lines for Electrical Quantities of a Mining Machine's Converter Power Supply System", *Energies*, 14, 2384, 2021.

[7] J. Karliński, M. Ptak and L. Chybowski, "Simulation-Based Methodology for Determining the Dynamic Strength of Tire Inflation Restraining Devices", *Energies,* 13(4), pp. 1-14, 2020.

[8] J. Karliński, M. Stańco, M and P. Działak, "Determination of the dynamic overloads in the loader structure", *Materials Today-Proceedings*, 4, 5, pp. 5843-5848, 2017.

[9] R. Waloski, W. Korzeniowski, Ł. Bołoz and W. Rączka, "Identification of Rock Mass Critical Discontinuities While Borehole Drilling", *Energies*, 14, 2748, 2021.

[10] P. Kamiński, A. Dyczko, and D. Prostański, "Virtual Simulations of a New Construction of the Artificial Shaft Bottom (Shaft Safety Platform) for Use in Mine Shafts", *Energies,* 14, 2110, 2021.

[11] J. Gajewski, P. Golewski and T. Sadowski, "The Use of Neural Networks in the Analysis of Dual Adhesive Single Lap Joints Subjected to Uniaxial Tensile Test", *Materials (Basel)*, 15, 14(2), 2021.

[12] J. Gajewski, J. Podgórski, J. Jonak and Z. Szkudlarek, "Numerical simulation of brittle rock loosening during mining process", *Computational Materials Science*, 43(1), pp. 115-118, 2008.

[13] P. Działak and J. Karliński, "Comparative examination of the trailer frame in accordance with UIC 596-5", *Materials Today-Proceedings*, 12, 2, pp. 416-422, 2019,

[14] W. Biały, Ł. Bołoz and J. Sitko, "Mechanical Processing of Hard Coal as a Source of Noise Pollution. Case Study in Poland", *Energies*, 14, 1332, 2021.

[15] K. Krzysztof, Ł. Bołoz, K. Mucha and T. Wydro, "The mechanized supporting system in tunnelling operations", *Tunnelling and Underground Space Technology*, 113, 2021.

[16] A. Kozłowski and Ł. Bołoz, "Design and Research on Power Systems and Algorithms for Controlling Electric Underground Mining Machines Powered by Batteries", *Energies*, 14, 4060, 2021.

[17] M. Ťavodová, D. Kalincová, M. Hnilicová and R. Hnilica, "The influence of heat treatment on tool properties mulcher", *Manufacturing technology*, 16, 5, pp. 1169-1173, 2016.

[18] Ł. Bołoz and W. Biały, "Automation and Robotization of Underground Mining in Poland". *Applied Science,* 10, 7221, 2020.

[19] J. Karliński, E. Rusiński and T. Lewandowski, "New generation automated drilling machine for tunnelling and underground mining work", *Automation in Construction*, 17, 3, pp. 224-231, 2008.

[20] A. Reński, "Investigation of the Influence of the Centre of Gravity Position on the Course of Vehicle Rollover", *24th Enhanced Safety of Vehicles Conference*, At: Gothenburg, Sweden, 2015.

[21] J. Wu, A. Guzzomi and M. Hodkiewicz, "Static stability analysis of non-slewing articulated mobile cranes", *Australian Journal of Mechanical Engineering*, 12, 2014.

[22] D. Fujioka, A. Rauch, W. Singhose and T. Jones, "Tip-Over Stability Analysis of Mobile Boom Cranes with Double-Pendulum Payloads", *Proceedings of the American Control Conference*, pp. 3136-3141, 2013.

[23] W. Kacalak, Z. Budniak and M. Majewski, "Modeling and simulation research of crane stability in the operating cycle (in Polish)", *Modelling in Engineering*, 34, pp. 47-56, 2017.

[24] G. Romanello, "A graphical approach for the determination of outrigger loads in mobile cranes", *Mechanics Based Design of Structures and Machines*, 2, pp. 767-780, 2020.

[25] T. Lei, J. Wang and Z. Yao, "Modelling and Stability Analysis of Articulated Vehicles." *Applied Science,* 11, 3663, 2021.

[26] S. Bako, "Stability Analysis of a Semi-Trailer Articulated Vehicle, A Review." *International Journal of Automotive Science And Technology*, 5, 2, pp. 131-140, 2021.

[27] A. Tota, E Galvagno and M. Velardocchia, "Analytical Study on the Cornering Behavior of an Articulated Tracked Vehicle", *Machines*, 9, 38, 2021.
[28] R. Majdan, R. Abrahám, K. Kollárová, Z. Tkáč, E. Matejková and L. Kubík, "Alternative Models for Calculation of Static Overturning Angle and Lateral Stability Analysis of Subcompact and Universal Tractors", *Agriculture*, 11, 861, 2021.
[29] M. Bietresato and F. Mazzetto, "Definition of the Layout for a New Facility to Test the Static and Dynamic Stability of Agricultural Vehicles Operating on Sloping Grounds", *Applied Science,* 9, 4135, 2019.
[30] L. Vita, D. Gattamelata and D. Pessina, "Retrofitting Agricultural Self-Propelled Machines with Roll-Over and Tip-Over Protective Structures", *Safety*, 7, 46, 2021.
[31] Ł. Bołoz and A. Kozłowski, "Methodology for assessing the stability of drilling rigs based on analytical tests", *Energies*, 14, 24, 8588, pp. 1-29, 2021.
[32] P. Dudziński and G. Sierzputowski, "Innovative universal vehicle for experimental tests on roll-over stability of off-road wheeled machines and vehicles", *Journal of KONES Powertrain and Transport*, 23, 4, pp. 93-98, 2016.
[33] G. Sierzputowski and P. Dudziński, "A mathematical model for determining and improving rollover stability of four-wheel earthmoving vehicles with arbitrary undercarriage system design", *Archives of Civil and Mechanical Engineering,* 20, 52, pp. 320-338, 2020.
[34] L. Xuefei, "Dynamic model and validation of an articulated steering wheel loader on slopes and over obstacles", *Vehicle System Dynamics*, 10, pp. 1305-1323, 2013.
[35] Xuefei L. "Research on lateral stability and rollover mechanism of articulated wheel loader", *Mathemathical and Computer Modelling of Dynamical Systems*, 5, pp. 248-263, 2014.
[36] L. Xuefei, W. Ya, Z. Wei, and Y. Zongwei, "Study on Roll Instability Mechanism and Stability Index of Articulated Steering Vehicles", *Mathematical Problems in Engineering*, 4, pp. 1-15, 2016.

Łukasz Bołoz
AGH University of Science and Technology
A. Mickiewicza Av. 30, 30-059 Krakow, Poland
e-mail: boloz@agh.edu.pl

Artur Kozłowski
Łukasiewicz Research Network – Institute of Innovative Technologies EMAG
ul. Leopolda 31, 40-189 Katowice, Poland
e-mail: artur.kozlowski@emag.lukasiewicz.gov.pl

Wojciech Horak
AGH University of Science and Technology
A. Mickiewicza Av. 30, 30-059 Krakow, Poland
e-mail: horak@agh.edu.pl